Real-time displacement measurement using VCSEL interferometer

Takamasa Suzuki*[a], Noriaki Yamada[a], Osami Sasaki[b], and Samuel Choi[b]
[a]Graduate School of Science and Technology, Niigata University, 8050, Igarashi 2, Niigata, 950-2181, Japan; [b]Faculty of Engineering, Niigata University, 8050, Igarashi 2, Niigata, 950-2181, Japan

ABSTRACT

A displacement sensor that uses a vertical cavity surface emitting laser (VCSEL), which is superior in terms of remediation of the mode-hop issue and modulation efficiency, is proposed. The interference signal in the sensor is processed with the phase-locked technique. This device allows real-time measurement of displacement. No unstable signals due to mode-hop were observed in the experiments. Displacement measurements recorded with this device indicated that it has an rms measurement accuracy of 0.3 μm and 50 nm for displacements of 150 μm and 1.2 μm, respectively.

Keywords: displacement sensor, laser diode, interferometer, vertical cavity surface emitting laser diode

1. INTRODUCTION

Displacement sensors (DSs) are among the most important devices used in high-precision manufacturing. They monitor the thermal expansion of rotating spindles and ball screws, the position of cutters, vibrations caused by misalignment of rotating objects, and other such parameters. Such sensors need to be compact and robust against mechanical disturbances in manufacturing processes.

There are many types of noncontact DSs such as ultrasonic, capacitance, eddy current, and optical DSs. Optical DSs are easy to use, applicable to most materials, and have high accuracy. Optical DSs are categorized into two types based on the measurement principle used, namely, triangulation- and interferometry-type DSs. Because the resolution of triangulation-type DSs is inadequate, interferometry-type DSs are suitable for ultraprecision machining. However, an interferometer is typically expensive and unstable because of the mode-hop phenomenon when a conventional Fabry-Perot laser diode (LD) is used in it as a light source. Moreover, the poor wavelength tunability of a conventional LD restricts the measurement range of the sensor.

The interferometer we propose herein uses a vertical cavity surface emitting laser (VCSEL). It is superior in terms of remediation of the mode-hop issue and modulation efficiency. Also, it is adaptable for high-speed modulation and is insensitive to temperature changes. Furthermore, the cleavage process, which is required in fabricating conventional LDs, is not necessary in a VCSEL. The fabricating cost of the VCSEL can be reduced because of the simplified quality control. The low power consumption and low fabrication cost of the VCSEL makes its use cost-effective.

Because the interference signal is processed with the phase-locked technique, this device allows real-time measurement of displacement. No unstable signals due to mode-hop were observed in the experiments. Displacement measurements recorded with this device indicated that it has an rms measurement accuracy of 0.3 μm and 50 nm for displacements of 150 μm and 1.2 μm, respectively.

2. PRINCIPLE

2.1 Wavelength tunability of the light sources

The properties of wavelength tunability by current injection in a conventional LD and a VCSEL are shown in Figs. 1(a) and 1(b), respectively. They indicate that the wavelengths in both devices can be modulated by injection current. This property is very useful for configuring a real-time DS. However, the modulation efficiency β of the VCSEL is very large in comparison with the LD. Additionally, no mode-hop phenomenon was observed in the VCSEL. These special properties of the VCSEL are advantageous in configuring a stable sensor with a wide measurement range.

*takamasa@eng.niigata-u.ac.jp; phone / fax 81 25 262-7215

Optical Metrology and Inspection for Industrial Applications II, edited by Kevin G. Harding, Peisen S. Huang, Toru Yoshizawa, Proc. of SPIE Vol 8563, 85630K · © 2012 SPIE
CCC code: 0277-786/12/$18 · doi: 10 1117/12.999720

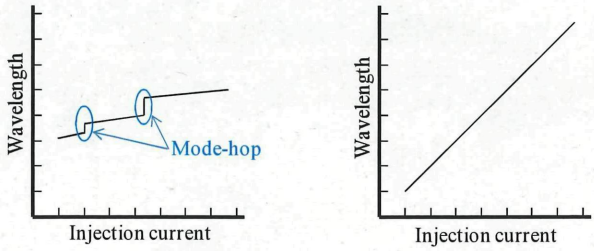

(a) Conventional LD (b) VCSEL

Fig. 1 Wavelength tunability of the conventional LD and VCSEL.

The main specifications of the two sources are presented in Table 1. The modulation efficiency of the VCSEL is about hundred times greater than that of a standard LD, although its power and current requirements are lower.

Table 1 Comparison between the VCSEL and conventional LD.

	VCSEL ULM763 (U-L-M Photonics)	LD HL6326G (HITACHI)
Wavelength	763 nm	635 nm
Output power	0.25 mW	10 mW
Operating current	2.0 mA	40 mA
Threshold current	0.5 mA	30 mA
Modulation efficiency	0.5 nm/mA	0.005 nm/mA

2.2 Phase compensation with a feedback control

We used phase-locked LD (PLLD) interferometry, in which the phase of an interference signal is compensated with a feedback control, to measure displacement. A large modulation efficiency is advantageous in the PLLD interferometry because it involves controlling the phase via wavelength tuning.

If the light source is modulated with a sinusoidal signal

$$i_{\mathrm{m}}(t) = a\cos(\omega_c t + \theta), \tag{1}$$

a sinusoidal phase modulating signal[6]

$$\begin{aligned} S(t) &= S_1 + S_0\cos\left[z\cos(\omega_c t+\theta)+\alpha(t)\right] \\ &= S_1 + S_0\cos\alpha(t)\left[J_0(z) - 2J_2(z)\cos 2(\omega_c t+\theta)+\cdots\right] \\ &\quad - S_0\sin\alpha(t)\left[2J_1(z)\cos(\omega_c t+\theta) - 2J_3(z)\cos 3(\omega_c t+\theta)+\cdots\right] \end{aligned} \tag{2}$$

is obtained, where z and $\alpha(t)$ are, respectively, the deviations in the modulation depth and temporal phase due to the displacement, respectively. They are given by

$$z = \frac{4\pi a\beta L_0}{\lambda_0^{\,2}} \tag{3}$$

and

$$\alpha(t) = \frac{4\pi L_0}{\lambda_0} + \frac{4\pi d(t)}{\lambda_0}, \tag{4}$$

respectively, where $2L_0$ is the optical path difference, and $d(t)$ is the displacement.

When $S(t)$ is multiplied by $i_m(t)$ and the product is passed through a low-pass filter, we can obtain the feedback (FB) signal[7]

$$Y_s(t) = A_s \sin\alpha(t), \tag{5}$$

where A_s is the amplitude depending on S_0 and $J_1(z)$. This process is called synchronous detection. Figure 2 illustrates the FB signal $Y_s(t)$. If the phase deviates due to the displacement of the object, the operating point moves along the FB signal. The operating point, however, returns to its original position when the FB control works properly. This phase compensation is made within the stable area. If negative FB is activated at the positive slope of $Y_s(t)$, the FB loop is stable. On the other hand, the FB loop becomes unstable at the negative slope[8].

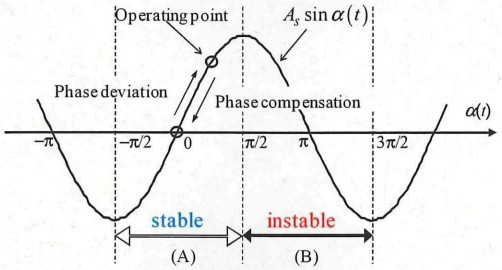

Fig. 2 Schematic of the feedback signal.

2.3 Phase-locked interferometry

In PLLD interferometry, the FB controller changes the wavelength λ_0 by λ_c using the wavelength tunability of the LD. The phase shown in Eq. (4) is then changed to

$$\alpha_c(t) = \frac{4\pi\left[L_0 + d(t)\right]}{(\lambda_0 + \lambda_c)} = \frac{4\pi L_0}{\lambda_0} + \frac{4\pi d(t)}{\lambda_0} - \frac{4\pi L_0}{\lambda_0^2}\lambda_c(t). \tag{6}$$

Because the phase maintained at the initial value $4\pi L_0/\lambda_0$, the last term of the control cancels out the second term. Thus, the displacement is given by

$$d(t) = \frac{L_0}{\lambda_0}\lambda_c(t) = \frac{L_0}{\lambda_0}\beta i_c(t), \tag{7}$$

where $i_c(t)$ is the control current.

3. EXPERIMENTS

3.1 Experimental setup

A schematic of our system is illustrated in Fig. 3. Light irradiated from a VCSEL was fed into a two-beam interferometer. The optical path difference $2L_0$ was 60 mm. Characteristics of the VCSEL are shown in Table 1. We used a mirror mounted on a piezoelectric transducer (PZT) as the measured object. The interference signal detected by a photodetector (PD) was fed to the feedback controller (FBC). The dc bias current I_0, modulating current $i_m(t)$, and control current $i_c(t)$ generated in the FBC were injected into the VCSEL. The modulation frequency of $i_m(t)$ was 10 kHz. The control current was monitored by a computer so as to measure the displacement of the object.

Figure 4 shows the block diagram of the FBC. The multiplier (MUL) and low-pass filter (LPF) implement synchronous detection, as explained in the previous section. Because the cut-off frequency of an LPF is typically selected as 1/10 of

the modulation frequency, it was set to 1 kHz. The error signal $e(t)$, which was generated by comparing the reference signal r_0 and feedback signal $Y_s(t)$, was fed into the proportional-integral (PI) controller.

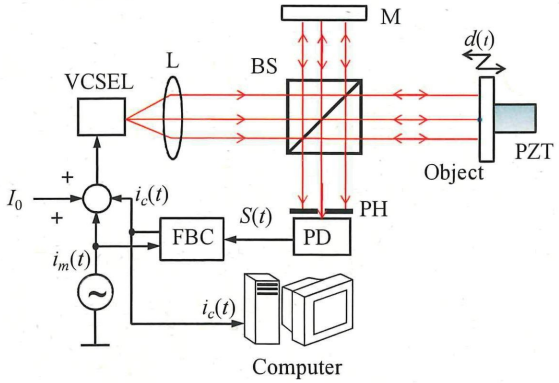

Fig. 3 Experimental setup. L, lens; BS, beamsplitter; PH, pinhole; PD, photodetector; FBC, feedback controller.

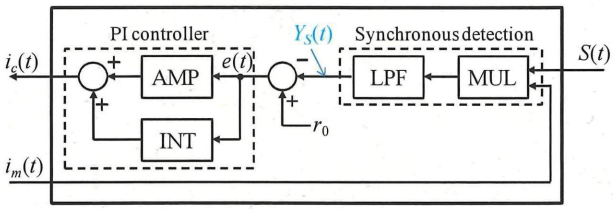

Fig. 4 Block diagram of the FBC. AMP, amplifier; INT, integrator; LPF, low-pass filter; MUL, multiplier.

3.2 Experimental results

We measured two kinds of displacement— discrete and continuous—produced by the PZT being driven by dc and ac voltage, respectively, as shown in Fig. 5(a) and 5(b).

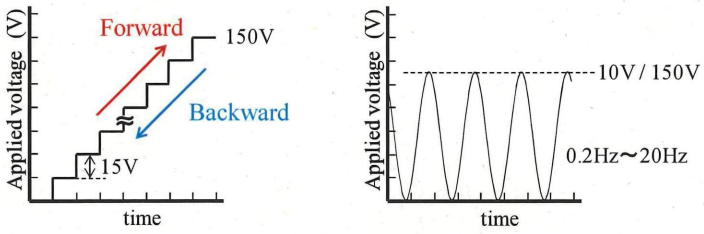

Fig. 5 Waveforms of the voltage applied to the PZT.

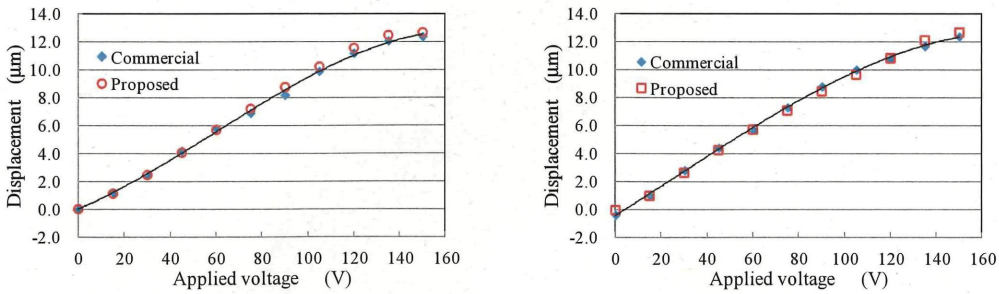

Fig. 6 Discrete displacement of the object: (a) forward and (b) backward.

The discrete forward and backward displacements are traced in Fig. 6(a) and 6(b), respectively. The voltage was applied up to 150 V in increments of 15 V. The squared markers show the results obtained using a commercial DS with a resolution of 0.1 μm. The solid line is the fitted curve. Although the measurements started from the position at an applied voltage of 0 V in Fig. 6(a) and ended at the initial position in Fig. 6(b), the trajectories differed slightly because of the hysteresis characteristic of the PZT. Comparing these results with those of the commercial sensor, the rms measurement errors in Figs. 6(a) and 6(b) were estimated at 0.28 mm and 0.25 mm.

Next, we measured some continuous displacements using a sinusoidal driving signal. Figures 7 and 8 were obtained when the maximum applied voltage was set to 10 V. The frequencies of the signals are 1 Hz and 10 Hz, respectively, in Figs. 7 and 8. Figures 7(a) and 8(a) show the displacement measured with the commercial DS. While the results traced in Fig. 7(b) show good agreement with those in Fig. 7(a), they differs from those in Fig. 8. The amplitude and phase of the displacement shown in Fig. 8(b) are smaller and delayed, respectively, compared with those in Fig. 8(a). This was attributed to the response property of the integrator in the PI controller. The gain-phase characteristic of our system is shown in Fig. 9. It seems that the accuracy of the proposed system degrades at frequencies above 1 Hz. The cut-off frequency can be calculated as 14 Hz from Fig. 9(a). This means that the time constant in our system is 0.07 s. In our prototype, we set the time constant to be slightly longer than that in the commercial sensor so that the feedback control became quite stable. It is believed that the frequency response could be improved by properly adjusting the control parameter.

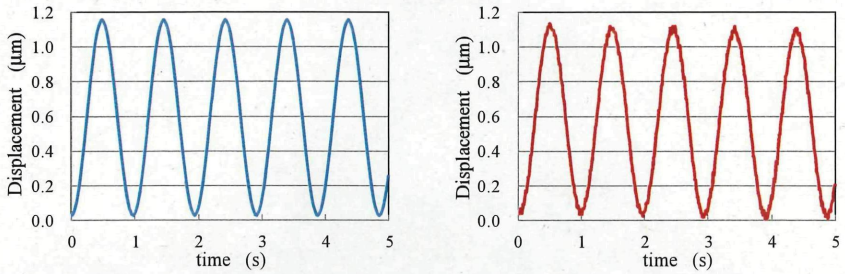

Fig. 7 Continuous small displacement (1 Hz) measured with (a) the commercial device and (b) the proposed system.

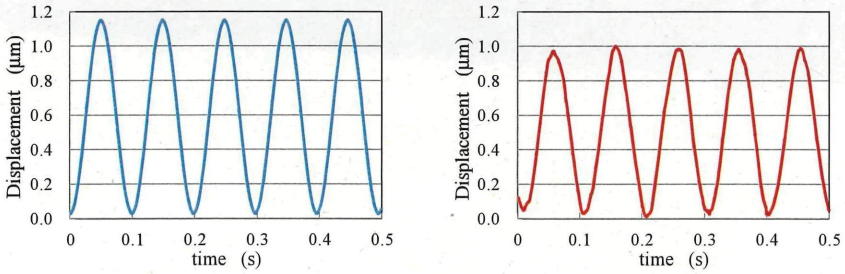

Fig. 8 Continuous small displacement (10 Hz) measured with (a) the commercial device and (b) the proposed system.

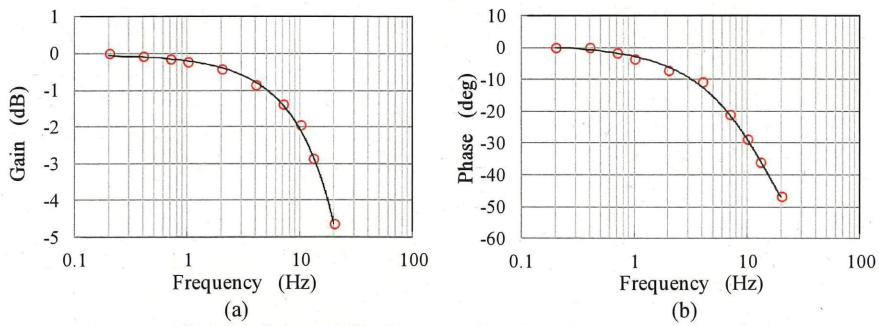

Fig. 9 (a) Gain and (b) phase as a function of frequency.

Finally, a large displacement was measured. We applied a sinusoidal voltage with an amplitude of 150 V_{p-p} and a frequency of 0.2 Hz to the PZT. The results, shown in Figs. 10(a) and 10(b), were obtained with the commercial device and proposed one, respectively. They confirmed that the prototype can measure a large displacement of 17 μm accurately in the low-frequency region. From the difference between Figs. 10(a) and 10(b), the rms measurement error was calculated as 0.3 μm. The maximum measurement range was estimated to be 25 μm under the experimental conditions used in the present paper. This range was limited by the output range of the integrator.

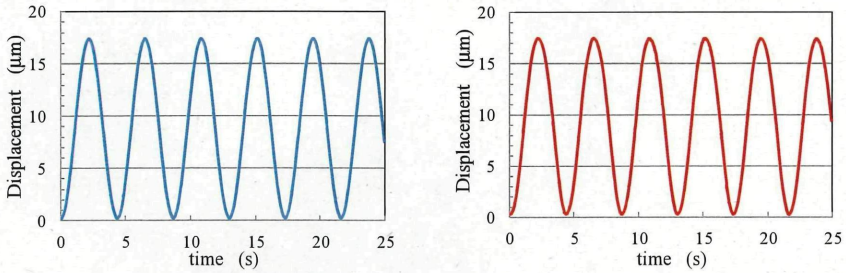

Fig. 10 Continuous large displacement (0.2 Hz) measured with (a) the commercial device and (b) the proposed system.

4. CONCLUSIONS

A real-time displacement sensor that exploits the high modulation efficiency and stable oscillation property of a VCSEL was proposed and demonstrated. We confirmed that a large measurement range can be obtained using a VCSEL. The response property, however, needs to be improved, and this may be achieved by adjusting the control parameters. After such calibration, we can expect to realize a high-precision real-time displacement sensor at low cost.

REFERENCES

[1] Information guide from KEYENCE, "Displacement Sensors," <http://www.sensorcentral.com/displacement/laser02.php>

[2] Suzuki, T., Sasaki, O., Higuchi, K. and Maruyama, T., "Real-time displacement measurement in sinusoidal phase modulating interferometry," Appl. Opt., 28(24), 5270-5274 (1989).

[3] Tatsuno, K. and Tsunoda Y., "Diode laser direct modulation heterodyne interferometer," Appl. Opt., 26(1), 37-40 (1987).

[4] Koyama, F., "Recent advances in VCSEL photonics," J. Lightwave Technol., 24 (12), 4502-4513 (2006).

[5] Suzuki, T., Sasaki, O., Takeo, M., "Phase-locked laser diode interferometry for surface profile measurement," Appl. Opt., 28(20), 4407-4410 (1989).

[6] Sasaki, O., Takahashi, K., Suzuki, T., "Sinusoidal phase modulating laser diode interferometer with a feedback control system to eliminate external disturbance," Opt. Eng., 29(12), 1511-1515 (1990).

[7] Suzuki, T., Sasaki, O., Takayama S., Takeo, M., "Real-time displacement measurement using synchronous detection in a sinusoidal phase modulating interferometer," Opt. Eng., 32(5), 1033-1037 (1993).

[8] Suzuki, T., Takahashi, T., Sasaki, O., Takeo, M., "Disturbance-free phase-shifting laser diode interferometer using adaptive feedback control," Appl. Opt., 48(31), 5561-5566 (2009).